Proceedings of International Conference on Heat Exchanger Fouling and Cleaning - 2011 (Peer-reviewed)
June 05 - 10, 2011, Crete Island, Greece
Editors: M.R. Malayeri, H. Müller-Steinhagen and A.P. Watkinson

Published online
www.heatexchanger-fouling.com

GROWTH RATES OF DRY PARTICULATE FOULING UNDER VARIABLE PROCESS CONDITIONS

K. K. Sathyanarayanarao Subbarao, C. C. M. Rindt and A. A. van Steenhoven

Faculty of Mechanical engineering, Energy technology group
Eindhoven university of technology, Post box 513, 5600MB, The Netherlands
k.kiran@tue.nl

ABSTRACT

Particulate Fouling is a complex phenomenon and is governed by various process conditions. It is imperative to elucidate the effects of individual parameters governing the fouling process for better understanding and to aid in numerical modeling. Most of the experimental studies on fouling involve in-situ measurements in the process plants where the individual effects of process conditions are difficult to evaluate. Controlled lab scale experiments that have been reported are limited to a few. In this direction, a controlled high temperature experimental facility has been built to study dry particulate fouling under varying process conditions. Experiments have been conducted for a range of process parameters like: gas phase velocity, particle size distribution, particle mixtures, deposition probe materials and geometries. An optical technique is developed to measure the evolution of fouling layer growth with time. The particle deposition and fouling layer growth is measured for a single cylinder to avoid the complexities associated with the flow dynamics of multiple tube arrays. It is found that the gas phase velocity plays a vital role in the overall process. Experiments with a square tube with its sides inclined at various angles to the mainstream flow direction indicated a reduction in deposition. A cylindrical tube oriented at an angle to the flow also indicated reduced fouling tendency. The geometry of the heat exchanger tube influences the deposition process and by modifying the geometry dry particulate fouling can be reduced.

INTRODUCTION

Background

The flue gases emanating from different processes like coal combustion, biomass gasification etc inevitably contains particulate matter. The process of deposition of particulate matter on heat exchanger surfaces is known as particulate fouling. The deposited particles eventually form a layer of very low thermal conductivity and reduce the heat transfer efficiency of the heat exchanger system. Fouling also leads to huge maintenance and capitals costs. A review of fouling and its implications on system costs and efficiencies has been reported by several researchers; Epstein (1983), Somerscales (1990) and Bryers (1996). Van Beek et al. (2001) have analyzed fouling in refuse waste incinerators and report that the fouling layers varied from thin powdery layers in the economizer section to thick and sintered layers in superheater section of the boiler. They report that each type of fouling layer resulted in a reduction of around 27% in the overall heat transfer coefficient even though the structure of the layers were different indicating the importance of powdery layers formed due to particulate fouling. Baxter and DeSollar (1993), van Beek et al. (2001) and others have reported that fouling resistance curve displays an asymptotic behavior. As fouling resistance is directly related to the fouling layer characteristics, a similar asymptotic behavior in fouling layer thickness is expected which indicates a balance between the rate of deposition and removal as proposed by Kern and Seaton (1959). The exact mechanisms for the asymptotic behavior are however still not clear. Experimental efforts towards understanding and controlling fouling have been made my many researchers, e.g. Bohnet (1987), Kaiser et a.l (2002), Kalisz and Pronobis (2005), Hupa (2005) and Abd-Elhady et al (2009). Muller-Steinhagen et al (1988) and Grillot and Icart (1997) have reported that fouling is strongly governed by the flow velocity. Abd-Elhady et al. (2004) suggested that fouling can be avoided if the gas speed is maintained larger than the critical flow velocity. Critical flow velocity is defined as the minimum flow speed necessary to roll a particle resting on a flat surface. An influence of flow direction on particulate fouling was observed by Abd-Elhady et al. (2009) and it was reported that fouling starts at the stagnation region and the best orientation for reduced fouling is a downward flow. Kaiser et al. (2002) have reported that humidity and tube bundle geometry plays a major role on the overall deposition pattern of particulate matter and suggested further experiments with different foulants, different tube geometry and surfaces for better understanding. Kim et al. (1992) report that thermophoretic effects dominate sub micrometer sized particle deposition and inertial impaction dominates the deposition mechanism for bigger particles.

Experimental data cited in the literature mainly correspond to the measured particle deposition rates in real heat exchangers systems. Though these experiments are vital in their own respect, they cannot fully serve to help understand and model particle deposition from a fundamental view point. This is mainly due to the fact that particle deposition in real systems is a complex process involving many factors. This includes particle composition, chemical reactions, condensation of vaporized species on the heat exchanger tubes, sintering effects and process conditions. Lab scale experiments that have been reported are limited and many of them mimic real systems (like entrained reactors) where many parameters are lumped together.

Aim of the present study

A detailed parameterized study on particle deposition is thought to be of crucial importance to gain insight into the fouling process and to provide data for simple modeling of particle deposition over tubes. The aim of the present study is to perform qualitative and quantitative analysis of the parameters governing dry particulate fouling. The effect of particle concentration, flow velocity, gas phase temperature, material properties of the foulants and tube geometries are studied experimentally to understand fouling tendency and to provide quantitative temporal data of particle deposition.

EXPERIMENTAL FACILITY

Setup

An experimental facility to perform controlled experiments on particulate fouling has been built and tested for its operational ability and repeatability. The controlled fouling experimental setup is shown in Figure 1. The experimental facility is a vertically oriented closed loop wind tunnel and consists of different parts interconnected by stainless steel ducting. A short description of the operating principle and measuring technique is described here. More details regarding the experimental setup can be found in earlier work, Sathyanarayanarao Subbarao et al. (2009). The blower maintains the required flow rate ranging from 0.08 - 0.2 m^3/s. The air then passes through a diverging duct to enter the electric heater where it is heated to the required temperature by several electric heating coil elements. The hot air from the heater passes through the ducting which consists of a straight section and two 90^o bends by which the motion of air is changed from upward to downward direction. A combination of vanes, grids, diverging and converging zones are used to condition the flow soon after the second bend. A particle screw feeder positioned on the top of the setup discharges the required amount of particles into the flow in a tube. The amount of particles seeded into the flow can be controlled by regulating the speed of the stepper motor of the screw feeder. The outlet of the particle seeding tube is positioned just at the turbulence grid at the centre of the duct. The seeding position was chosen based on several flow and particle tracking simulations in order to obtain a quasi-homogeneous particle distribution. The test section is positioned 2 m below the particle inlet to allow sufficient distance for the flow to develop and to provide sufficient residence time for the particles in the hot air so that the particles can attain a quasi thermal equilibrium state with the gas phase. The velocity and temperature of the air is measured 100 mm above the deposition tube by a Pitot tube with an integrated thermocouple. The deposition of the particles and their growth over a cylinder is observed in the test section which is provided with glass windows on three sides of the duct. The presence of three windows facilitates observation of the fouling layer from different sides. Beyond the test section, the hot air and the seeded particles move straight in the duct for 1.5 m downstream and then enter the cyclone separator through a 90^o bend. The bend is positioned 1.5 m away from the test section to avoid upstream disturbances. The outlet of the cyclone separator and the inlet of the blower are connected by circular tubing. Except for the transition zones, a square ducting of 200 x 200 mm cross section is used. At nominal conditions, the experimental facility can be operated for velocities in the range of 1.5 m/s to 5 m/s, temperatures from room temperature up to 500 ^oC and particle concentrations from 0.2 g/m^3 up to 20 g/m^3 depending on gas phase velocity and the type of parti

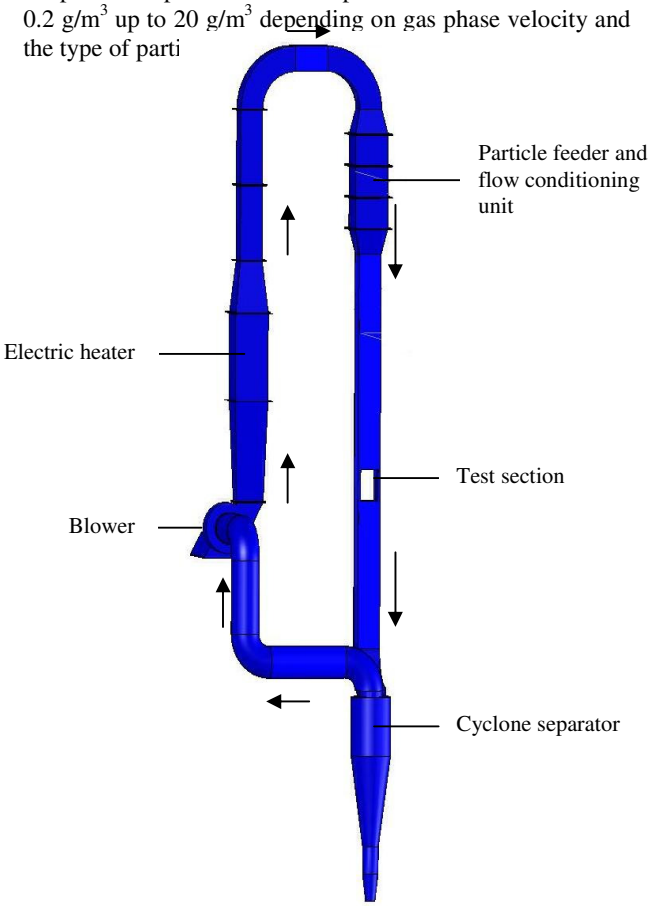

Figure. 1. Schematic of the controlled fouling experimental setup.

Measurement technique

To observe the process of fouling as a function of time, the test section is provided with glass windows on three sides which facilitate optical measurement of the fouled tube in axial and cross wise directions. A laser diode of 650 nm

[Roithner laser tecknik] which generates a sheet of 1 mm thickness is used perpendicular to the deposition tube and illuminates the region around the tube. The camera and the tube axis are in the same line but the camera is positioned above the axis of the tube in order to capture the layer growth. Figure 2a shows the deposition tube and the camera. Figure 2b shows the schematic of the laser sheet used to illuminate the region of interest. A Jai CV M10 CCD camera with a resolution of 600 x 400 pixels is used. A reference image is taken with a graph sheet to calibrate the image. Images of the tube are taken before, during and after the experiments. After the experiments, the deposition tube is carefully removed and the deposit thickness at the stagnation point is measured with a digital Vernier caliper to evaluate the thickness in order to compare with the image analysis. The difference in thickness between the two methods was found to be ± 3%.

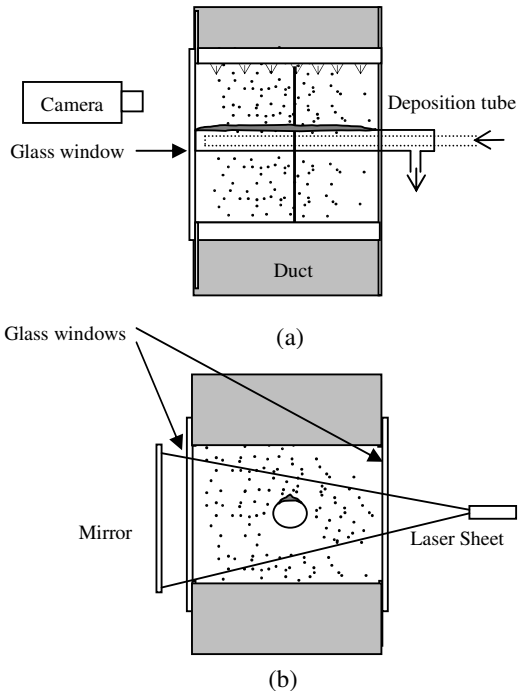

Figure. 2. Schematic of the test section.
a) View perpendicular to the deposition tube
b) View in line with the tube axis.

Materials and methods

Glass, Calcium Carbonate ($CaCO_3$) and Ash particles recovered from a Dutch biomass gasifier were used as foulant materials. Figure 3 shows the Scanning Electron Microscope (SEM) images of the foulant particles used. The glass particles ranged from 5 to 56 µm with a mean diameter of 20 µm and a standard deviation of 8 µm. The calcium carbonate particles ranged from 8 to 70 µm with a mean size of 40 µm and a standard deviation of 14 µm. The size of $CaCO_3$ particles was evaluated based on the longest side. The ash particles were composed of different shapes and sizes as shown in the SEM image. Most of the particles were like curled up flakes of length in the range of 100 to 150 µm. Smaller particles in the range of 20 to 50 µm were observed. Detailed analysis for the size distribution was not done.

The screw feeder was calibrated by weighing the output (g/minute) of the feeder under different motor speeds. This data was used to set the particle concentration in the flow based on the volumetric flow rate of air in the duct.

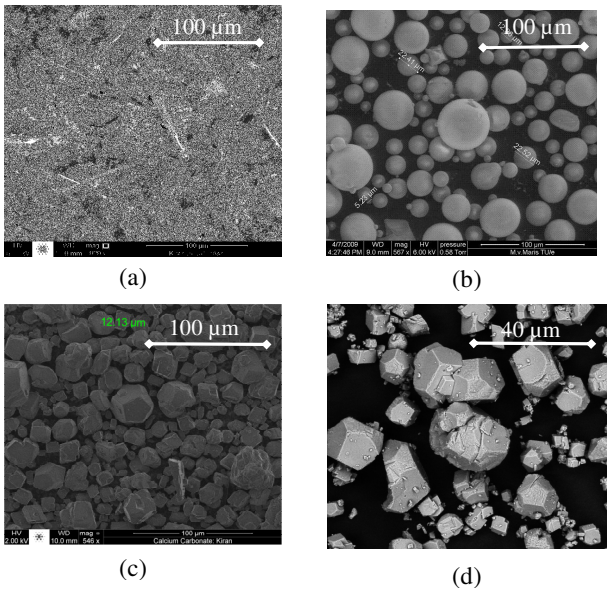

Figure. 3. SEM images of the particles used as foulants
(a) Ash. (b) Glass.
(c) & (d) $CaCO_3$

RESULTS

Ash deposition over a stainless steel tube

Figure 4 shows the layer growth dynamics for deposition of ash particles on a stainless steel tube of diameter 30 mm. Experiments were performed at nominal temperature, gas velocity (Vg) of 1.5 m/s and a particle concentration (Cp) of 0.2 g/m^3. The overlaid images with dark background in Figure 4 correspond to the raw images obtained for the clean tube and the fouled tube. The image overlaid on the bottom right is the processed image showing the evolution of the layer with time which is obtained by overlaying several transformed raw images over one another.

It is observed that deposition starts immediately when the flow is seeded with the particles. Particle deposition starts in the stagnation region and a simultaneous growth in radial and circumferential direction are observed. As time progresses, the radial growth rate is higher than the circumferential growth rate. The layer thickness in the stagnation line increases almost linearly but after 200 minutes of operation, the trend line flattens out indicating the onset of asymptotic behavior. A clear conical profile is formed with a sharp apex point. The experiment is continued until no further appreciable change in the layer thickness is observed for at least 100 minutes

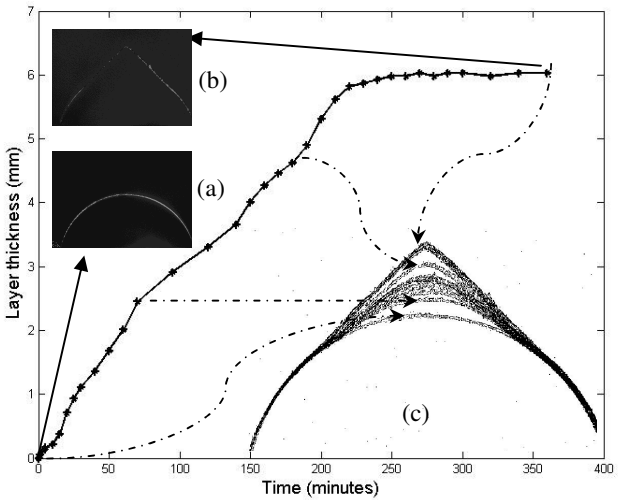

Figure. 4. Deposition of Ash particles over a stainless steel tube (Vg=1.5 m/s, Cp = 0.2 g/m^3),
(a) Raw image of the clean tube. (b) Raw image at the end of experiment and (c) Processed image

The axial distribution of ash particles can be seen in Figure 5b. A clearly distinguishable clean tube is seen which represents the region where the flow shear is maximum.

.

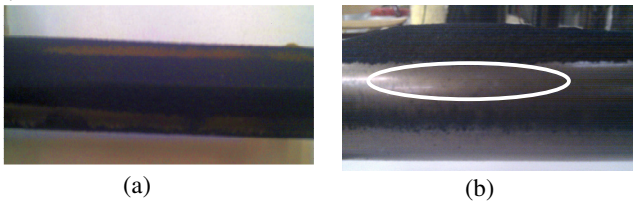

(a) (b)

Figure. 5. Snapshot of ash deposition pattern at the end of experiments. (a) Top view. (b) Side view (region of high shear rate is encircled). Black color corresponds to ash particles and the gray color refers to the tube.

Below this region a band of ash particles can be seen on the tube. This represents the region just after the flow detachment point. The width of the layer formed can be seen in Figure 5a which is uniform over the length of the tube. The tube was inspected at the bottom and no deposition was found.

Influence of gas phase velocity

It has been reported by several authors [Muller-Steinhagen et al. (1988), Grillot and Icart (1997)] that the shear force acting on the particles due to the flow influences the deposition to a large extent. Abd-Elhady et al. (2004) have reported that fouling ceases if the velocity of the gas phase is more than the critical velocity of the smallest particles in the flow based on the rolling moment theory for particle removal. Though it is evident that increasing the velocity reduces fouling tendency, there is a need to understand the relationship between small changes in velocity to that of fouling behavior.

In the present work, an effort has been made to capture the growth dynamics of the layer thickness and to correlate the change in deposition pattern to the gas phase velocity. Figure 6 shows the evolution of deposit layer thickness at the stagnation line for glass particles depositing over a stainless tube of 30 mm diameter. The particle concentration in each experiment was maintained at 2 g/m^3. The centre line thickness increases monotonically for the period where the deposition rates are more than the removal rate. The layer thickness reaches a constant value after certain duration showing an asymptotic behavior where the particle deposition and removal rates are balanced.

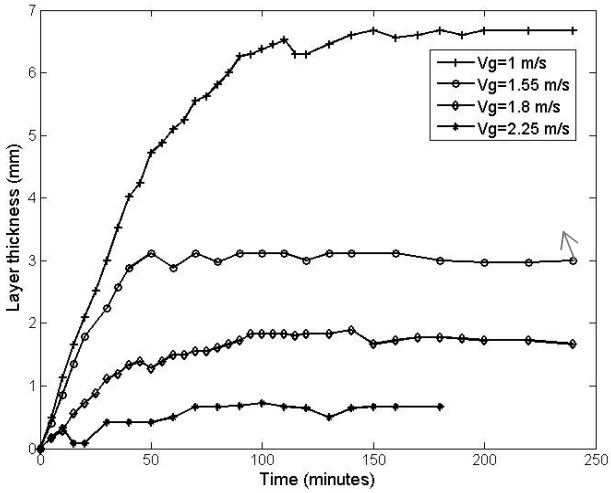

Fig.6. Effect of gas velocity on glass particle deposition on a stainless steel tube of diameter 30 mm. (Cp = 2 g/m^3)

The layer thickness at the stagnation point for Vg = 1 m/s was observed to be 6.7 mm. Increasing the flow velocity from 1 m/s to 1.5 m/s resulted in a lower growth rate and the overall thickness at the stagnation point reached was 3.15 mm. Thus a small increase in the velocity resulted in almost half the thickness. The circumferential growth was also found to be correspondingly less at higher velocity. For a flow velocity of 1.8 m/s, the overall thickness at the stagnation point further reduced to 1.8 mm and for a flow velocity of 2.25 m/s the thickness was found to be a maximum of 0.73 mm. Increasing the gas velocity to 2.5 m/s resulted in no deposit formation and the tube remained clean.

Figure 7 shows the deposition of calcium carbonate particles over stainless steel tube for different velocities with 2 g/m^3 of particle concentration in the flow. The general trend in the variation of fouling layer thickness with time is similar to the trend observed for glass particle deposition. However, the layer structure formed at the end of the experiment was different from that of glass and ash particles.

The maximum layer thickness at the centre was found to be 8.2 mm when the velocity was 1.5 m/s. Doubling the velocity to 3 m/s resulted in a layer thickness of 2 mm. The deposition at the maximum speed limit of the experimental setup of 5 m/s was found to be 0.5 mm.

Figure 8 shows the fouling behavior of a glass and $CaCO_3$ particle mixture (50:50 by weight). The waviness in the plot indicates the fall-off and re-growth of the layer. The thickness of the layer is larger than the thickness observed for glass particles at same velocity and smaller than the one for $CaCO_3$ particles. It is anticipated that the non spherical particles of $CaCO_3$ provide better sites for the deposition of spherical particles and thus has a faster growth in the initial stages. However, this needs further analysis to explain the behavior.

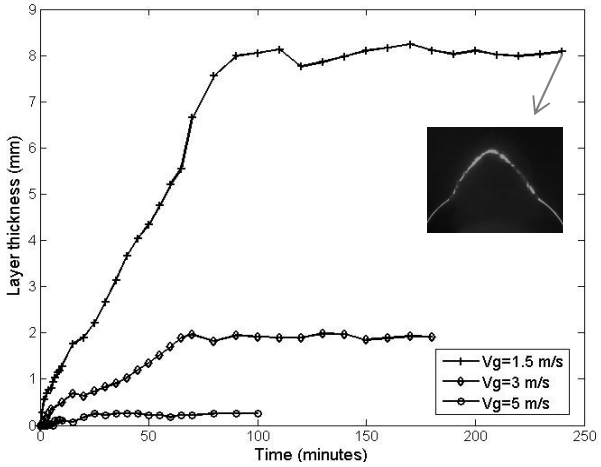

Figure. 7. Effect of gas velocity on $CaCO_3$ particle deposition (D_{tube} = 30 mm, Cp = 2 g/m^3).

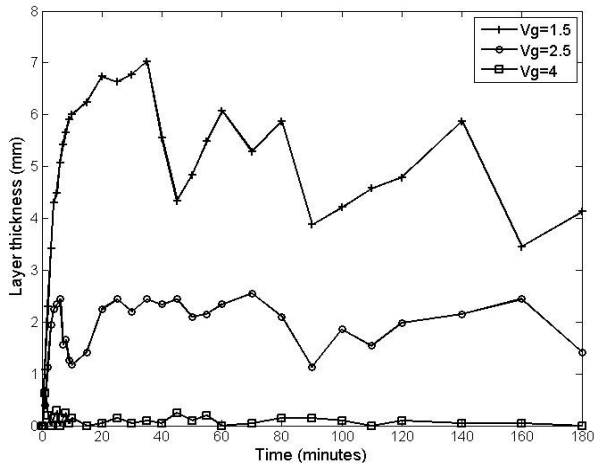

Figure. 8. Effect of gas velocity on $CaCO_3$ and glass mixture (D_{tube} = 30mm, Cp =2 g/m^3, mixture 50:50 by weight).

Mass deposition measurements

Experiments were done to evaluate the mass deposition over the cylinder with $CaCO_3$ particles to understand the particle deposition initiation period and to correlate the deposited mass to the shape of the fouling layer. Figure 9 shows the mass of the particles that deposit on a stainless steel cylinder. The gas velocity was maintained at 1.55 m/s and the particle concentration was maintained at 2 g/m^3 of air. The cylinder was inserted in the flow for a specific amount of time and was taken out. The deposited particles were carefully collected with a small artist's brush to minimize the loss of particles. The collected particles were weighed on a precision weighing machine with a least count of 1mg. A mean value for 5 tests performed for each time interval is reported in order to average the error associated with insertion and removal of the deposition probe. It has been reported by earlier studies by Abd-Elhady (2004) that fine particles are most likely to stick first to the tubes as compared to the coarse particles as smaller particles have a higher sticking velocity [Roger and Reeds (1984)]. The sticking velocity corresponds to the maximum velocity beyond which a particle impacting a surface rebounds. The particles collected after the experiments were analyzed with a scanning electron microscope and it was observed that the smaller particles found in the sample collected after 10 seconds were more in number than for the samples collected at 60 seconds, thus confirming the earlier findings that smaller particles deposit first and aid the deposition of larger particles.

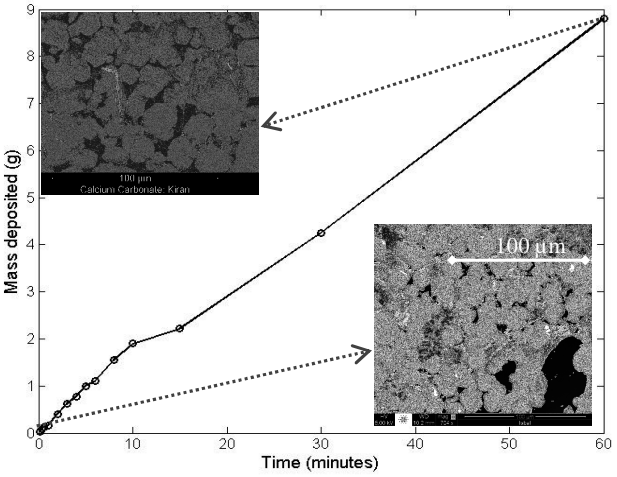

Figure 9. Mass deposition of $CaCO_3$ over a stainless steel tube (D_{tube} = 30 mm, Cp = 2 g/m^3).

The plot of mass deposition indicates a linear trend which increases monotonically up to 60 minutes of experimental duration, a similar trend as seen in the evolution of fouling layer thickness. The profile of the layer cross section and length of the tube being known, one can approximate the porosity of the layer formed. This can be used to calculate the fouling resistance of the layer as the thermal conductivity of the particles is known. However this needs information on the particle packing and the volume of the layer formed. The present work however has not evaluated these parameters.

Effect of gas temperature

Experiments with glass, $CaCO_3$ and polymer particles were performed at elevated temperatures in order to evaluate the effect of changes in gas phase viscosity and particle temperature on fouling behavior. Experiments were done at 250 ^{o} C and at 480 ^{o}C for glass particles maintaining the velocity similar to room temperature experiments. Glass

particles have a glass transition temperature of about 550 ^{o}C and $CaCO_3$ reacts at 550 ^{o}C to decompose and release Ca and CO_2. The material properties of both types of particles do not change drastically under these temperatures. However, the gas viscosity changes with temperature and hence the Reynolds number and the shear acting on the particles. The experimental observations indicated that the deposition pattern at higher temperatures were identical to the experimental observations for room temperature. This implies that the particle properties and the surface energies associated with the particle and the surface have a major role in the particle deposition process as compared to the viscosity of the gas phase.

Short duration experiments were performed with Ultra High Molecular Weight Poly Ethylene (UHMWPE) particles. After 10 minutes of operation (Tg = 22 ^{o}C, Vg=1.5 m/s, Cp = 0.25 g/m^3) a layer of 0.5 mm was formed. An experiment performed at 85 ^{o}C at which the particles soften indicated a layer thickness of 1.5 mm. The experiments with UHMWPE particles were limited to 10 minutes as the cyclone is inadequate to remove these particles and to avoid fouling of the duct work with polymers.

Effect of particle concentration:

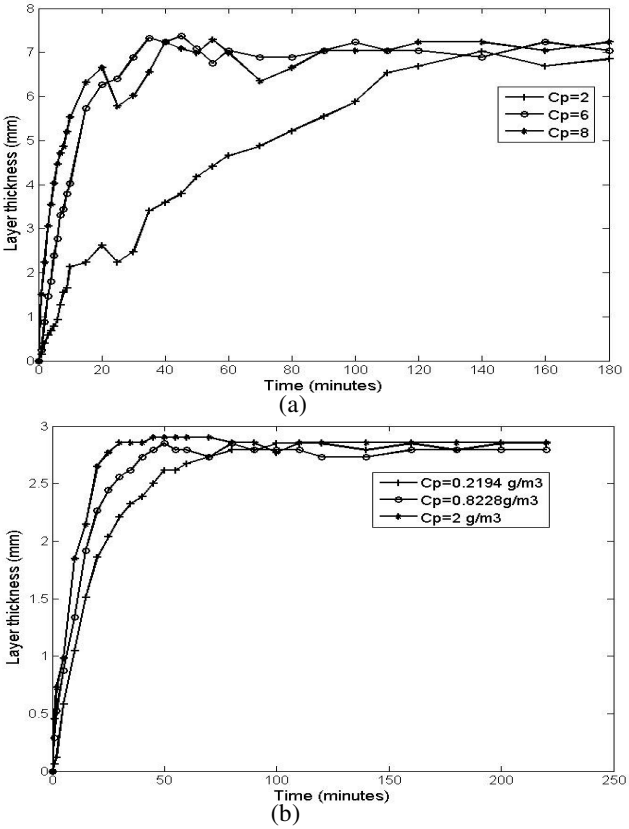

Fig. 10. Effect of particle concentration on particle deposition on cylinder.
a) $CaCO_3$ b) Glass

Suspended particulate matter in flue gases generally varies from a few mg/m^3 to 10 g/m^3 based on different process conditions, feedstock and heat exchanger section. Figure 10a and Figure 10b show the effects of varying particle concentration in the flow for experiments with $CaCO_3$ and glass particles for a gas phase velocity of 1.5 m/s. It is seen that an increasing particle concentration results in a faster growth rate of the layer but the overall layer thickness that eventually forms is more or less the same for all particle concentrations.

Effect of tube size

Glass particle deposition was studied for different target sizes. The stainless steel tubes used for deposition had similar roughness and were of 21, 30, 38 and 51 mm in diameter. Particle concentration was kept constant at 2.5g/m^3 in a gas flowing at a velocity of 1.5 m/s thus varying the Reynolds number based on the tube diameter.

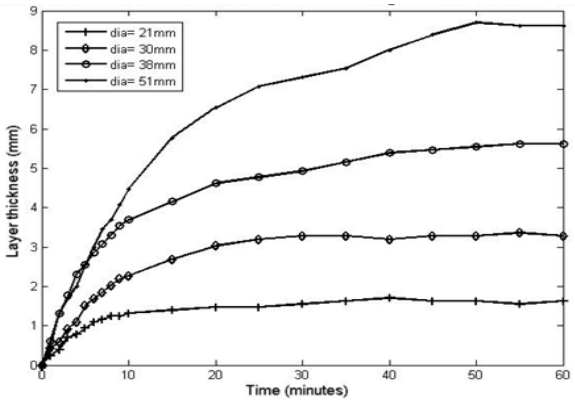

Figure 11. Deposition of glass particle on different tube sizes.

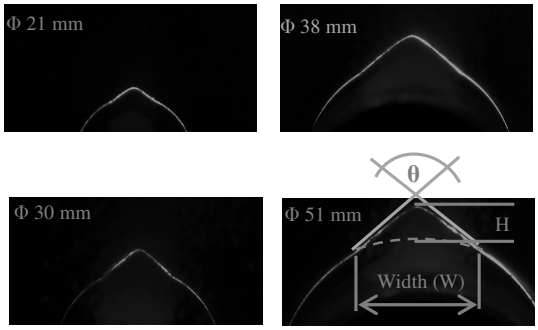

Figure 12. Glass deposition pattern for different tube diameters.

Table 1: Measured width (w), height (h) and angle (θ) on different tube diameters.

D (mm)	W (mm)	H (mm)	θ (deg)	H/W
21	6.5	1.62	117	0.249231
30	12.3	3.3	115	0.268293
38	20.3	5.4	116	0.26601
51	31	8.3	118	0.267742

Figure 11 shows the deposition pattern of glass particles on tubes with different diameters and Figure 12 shows the profile pictures taken at the end of each experiment.

Table 1 shows the measured height and width of the fouling layer at the end of the experiments. The ratio of height to width and the apex angle formed in each case was similar as shown in the table. The time for which the layer stops growing is also found to be proportional to the tube diameter. Varying the tube diameter results in different Reynolds numbers based on tube diameter and the blockage ratio [ratio of duct dimension to the tube diameter] also changes. The variation in Reynolds number and blockage ratio changes the wall shear stress acting on the cylinder wall and the overall boundary layer pattern on the cylinder. However, it is interesting to observe that though the flow features are affected, the deposition pattern seems to depend primarily on the geometrical and material properties.

Effect of tube geometry:

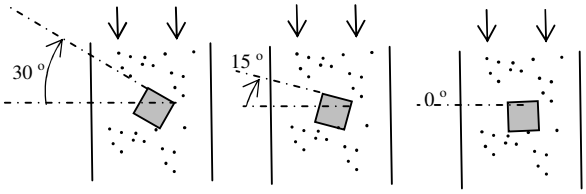

Figure 13. Orientation of square tube at different angles to the downward flow.

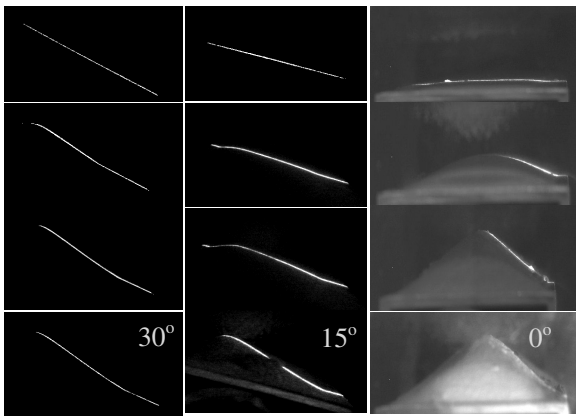

Figure 14. Deposition pattern of glass particles on a square tube oriented at different angles to the flow.

For a comparative study, a square geometry was selected and the face of the square tube was oriented in different angles to the flow shown schematically in Figure 13. The gas phase velocity was maintained at 1.5 m/s and particle concentration was 2 g/m^3. A square aluminum tube of side 40 mm was used as deposition target. Glass particle deposition patterns for angular orientations of 0^o, 15^o and 30^o are shown in figure 14. The straight line on the top left image represents the clean surface and the lower images shows the surface profile after particle deposition. It was observed that particle deposition starts in the region of stagnation of the flow for all the tube orientations. However, a tube oriented at 45 ^{o} to the flow remained clean for glass particles. The apex angle formed for all the orientations was between 115 ^{o} to 120 ^{o} and the apex forms at the stagnation region.

Effect of particle size

Glass particles of 20 µm mean diameter were mixed with a different set of glass particles with a mean diameter of 108 µm (50:50 by weight). An experiment with gas velocity of 1.5 m/s and particle concentration of 2g/m^3 resulted in no deposit formation. The tube remained clean after 2.5 hrs of experimentation. Larger particles have higher inertia and can knock off the smaller particles that have been already deposited over the cylinder surface thus leaving the surface clean. Figure 15a shows the snapshot acquired by a high speed camera for glass particles of 108 µm mean diameter flowing in air (Vg=1.5m/s). The particle tracks are straight indicating high inertia and the rebound process of a particle from the surface of the cylinder is seen. Figure 15b shows the particle paths for glass particles of mean diameter 20 µm. The trajectories of the particle follow the fluid and the extent to which small particles rebound is smaller than the rebound observed for larger particles.

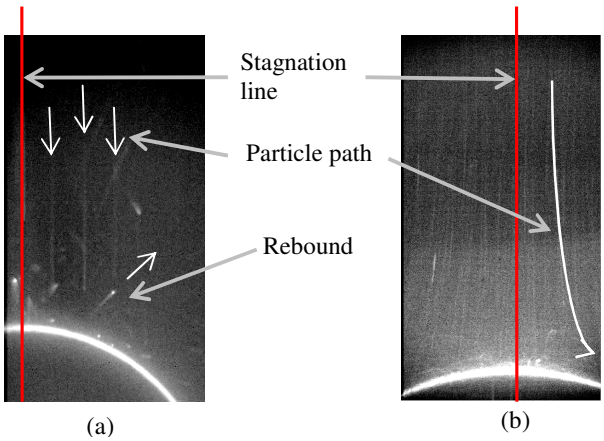

Figure 15. Image of glass particle impaction process over a cylinder recorded at 10 kHz.
(a) Glass particles (mean diameter 108 µm, Vg =1.5 m/s)
(b) Glass particles (mean diameter 20 µm, Vg =1.5 m/s)

DISCUSSION

Werner (1987) and Van Beek (2001) successfully showed that particle deposition can be modeled using a two-body collision model based on the Hertzian contact theory. According to the model, when a particle strikes another particle or a surface it can either undergo a elastic deformation or an elastic-plastic deformation based on the energy associated between the interacting bodies. If the adhesion energy overcomes the stored elastic energy, the particles "sticks" to the surface, else it rebounds. A detailed approach can be found in Van Beek (2001). For a particle impacting a surface at 90 ^{o}, the particle imparts all of its kinetic energy to the interaction mechanism. However, when a particle impacts a surface at an angle, only a component of the kinetic energy is dissipated in elastic plastic interactions. For oblique impactions, the tangential component of the particle creates a rotational component due to the friction between the particle and the surface. The resultant force acting on the surface is less compared to the normal incidence. Thus, a particle impacting the cylinder at the

stagnation line has a higher probability of sticking and a particle impacting away from the stagnation point has a lower probability of sticking. A particle which might rebound in the stagnation region is forced back to the cylinder surface due to the flow. Particles impacting the cylinder away from the stagnation point encounter an inclined plane and most of the kinetic energy is retained. Figure 15b shows the particle paths and interaction with the surface for glass particles of 20 µm. Thus, most of the initial particle growth occurs in the stagnation region. It was noted that for all experiments in the present study (all geometries and orientations) involving glass particles, an apex angle of approximately 120^o was formed and for $CaCO_3$ particles, the apex cone angle was 60^o. Abd- Elhady et al. (2011) reported that for $CaCO_3$ particles in their experiments, fouling was reduced by the inclusion of a cone shaped structure. They investigated the effect of different cone angles and found that 60^o angle reduced fouling the most. Comparing the present deposition pattern to their results, it can be concluded that a cone angle can be selected for different materials based on simple deposition experiment. To test the above explanation, A cylindrical tube oriented at 30^o to the flow was implemented as shown in Figure 16 and experiments were carried out with 2 g/m^3 of $CaCO_3$ particles. Deposition was not observed and the tube remained clean for 1 hr of operation for 5 m/s of gas velocity. The velocity was reduced to 4.5, 4, 3.5 and 3 m/s and the experiment was run for 1 hr for each speed. The tube remained clean for a gas phase velocity up to 3 m/s and deposition started at a velocity of 2.5 m/s. The layer thickness was 1 mm and remained constant for 1 hr of operation. In comparison to the straight orientation, the inclination of the tube resulted in lowering the fouling tendency and limiting velocity at which particle deposition begins. The inclination of the tube introduces two main characteristics: 1) the flow features are changed 2) the impaction of a particle normal to a surface is changed to oblique impactions. These two features seem to reduce the chances of particle adhering to the surface and hence results in reduced fouling tendency.

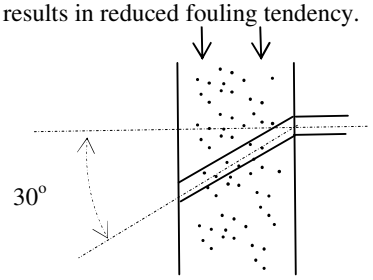

Fig. 16. Orientation of circular cylinder at 30^0 to the flow.

CONCLUSIONS

An experimental setup for performing controlled experiments on particulate fouling has been developed. A technique to measure the temporal evolution of fouling layer has been implemented which gives better insight into the process of particulate fouling.

It is conclusive that fouling tendency can be greatly reduced by increasing the flow speed.

The target geometry, orientation, particle-surface interaction and flow field are highly coupled and govern the overall deposition process. By altering the target geometry and orientation to the flow in a manner that normal impaction of particle with the surface is avoided helps to reduce particulate fouling.

FUTURE WORK

A numerical model based on two-body collision model for deposition and rolling moment model for particle removal is being developed. Further experiments into obtaining an optimal and feasible geometry and flow conditions are planned.

REFERENCES

Abd-Elhady, M. S., 2005, Gas-side particulate fouling in biomass gasifiers, PhD Thesis, Eindhoven University of Technology.

Abd-Elhady, M. S., Rindt, C. C. M and van Steenhoven, A. A., 2009, Optimization of flow direction to minimize particulate fouling of heat exchangers, *Heat Transfer Engineering*, 30 (10-11), 895-902.

Abd-Elhady, M. S., Rindt, C. C. M. and van Steenhoven, A. A., 2011, Influence of the apex angle of cone-shaped tubes on particulate fouling of heat exchangers. *Heat Transfer Engineering*, 32, (3 & 4), 272 – 281.

Abd-Elhady, M. S., Rindt, C. C. M. and van Steenhoven, A. A., 2004, Minimum gas speed in heat exchangers to avoid particulate fouling. International Journal of Heat and Mass Transfer, 47, 3943-3955.

Baxter, L. L. and DeSollar, R. W., 1993, A mechanistic description of ash deposition during pulverized coal combustion: predictions compared with observations, *Fuel*, Vol. 72, number 10, pp 1411-1418.

Bohnet, M., 1987, Fouling of heat-transfer surfaces, *Chemical engineering technology*, 10, 113-125.

Bryers, R. W., 1996, Fireside slagging, fouling and high temperature corrosion of heat transfer surface due to impurities in steam rising fuels. *Prog. Energy Combustion* Sci, 22:29-120.

Epstein, N., 1983, Thinking about heat transfer fouling: A 5 x 5 matrix, *Proc. 6th international heat transfer conference*, 235-253.

Grillot, J. M. and Icart, G., 1997, Fouling of a cylindrical probe and finned tube bundle in a diesel exhaust environment. *Experimental thermal and fluid science*, 14, 442-454.

Hupa, M., 2005, Interaction of fuels in co-firing in FBC, *Fuel,* 84, 2312-1319.

Kaiser, S., Antonijevic D. and Tsotsas E., 2002, Formation of fouling layers on a heat exchanger element exposed to warm, humid and solid loaded air streams. *Experimental thermal and fluid science*, 26, 291-297.

Kalisz, S. and Pronobis, M., 2005, Investigations on fouling rate in convective bundles of coal-fired boilers in relation to optimization of soot blower operation, *Fuel*, 84, 927-937

Kern, D. Q. and Seaton, R. E., 1959, A theoretical analysis of thermal surface fouling. *British Chemical Engineering,* 4(5), 258-262.

Kim, Y. J. and Kim, S. S., 1992, Experimental study of particle deposition onto a circular cylinder in high temperature particle laden flows, *Experimental thermal and fluid science*, 5, 116-123.

Muller-Steinhagen, H., Reif, F., Epstein, N. and Watkinson A. P., 1988, Influence of operating conditions on particulate fouling. *The Canadian journal of chemical engineering*, 66, 42-50.

Rogers, L. N. and Reed, J., 1984, The adhesion of particles undergoing an elastic-plastic impact with a surface, *J. Phys.D: Appl Phys*, 17, 677-689.

Sathyanarayanarao Subbarao, K. K., Rindt, C. C. M. and van Steenhoven, A. A., 2009, Preliminary study of particulate fouling in a high temperature controlled experimental facility, *Heat Exchanger Fouling and Cleaning*, Editors: H. Muller-Steinhagen et al., Schladming, Austria, 182-187,

Somerscales E. F. C., 1990, Fouling of heat transfer surfaces: An historical review. *Heat transfer engineering*, 11(1):19-36

Van Beek, M. C., Rindt, C. C. M., Wijers J. G. and van Steenhoven A. A., 2001, Analysis of fouling in refuse waste incinerators. *Heat transfer engineering*, 22: 22-31.

Van Beek, M. C., 2001, Gas-side fouling in heat recovery boilers, PhD thesis, Eindhoven University of technology.

Werner, B. T., 1987, A physical model of wind-blown sand transport, PhD Thesis, California institute of Technology